

# First principle study on the Structural and Electronic Properties of Lead-Free Double Halide Perovskite $\text{Cs}_2\text{InSbCl}_6$

Ahmad Zainab<sup>1</sup>, Magaji Ismail<sup>1</sup>, Alhassan Shuaibu<sup>1</sup> and Bashiru K Sodipo<sup>1</sup>

<sup>1</sup> Department of Physics, Faculty of Science, Kaduna State University, Kaduna, Kaduna State, Nigeria

Corresponding E-mail: [bashir.sodipo@kasu.edu.ng](mailto:bashir.sodipo@kasu.edu.ng)

Received 27-04-2023

Accepted for publication 10-05-2023

Published 11-05-2023

## Abstract

The structural and electronic characteristics of  $\text{Cs}_2\text{InSbCl}_6$  were investigated using first principle density functional theory (DFT) within local density approximation (LDA) and generalized gradient approximation (GGA) as implemented in the Quantum ESPRESSO package. A supercell with 40 atoms was used in carrying out the calculations, using the optimized lattice parameters of the  $\text{Cs}_2\text{InSbCl}_6$  ( $a = b = c = 11.342 \text{ \AA}$ ). The findings revealed that  $\text{Cs}_2\text{InSbCl}_6$  is a direct band gap material with gaps of 0.74 eV and 0.99 eV for LDA/PZ and GGA/PBE respectively, in which the GGA/PBE gap shows consistency within the literature range. The calculated densities of states highlight the contributions of the constituent atoms within the valence and the conduction bands.

Keywords: DFT; LDA; GGA; Lead free Perovskite  $\text{Cs}_2\text{InSbCl}_6$

## I. INTRODUCTION

Perovskites have unique features which make them suitable for application as photovoltaic absorbers [1]. These include high absorption coefficients, long carrier diffusion length, low exciton binding energy, tunable band gap, and low processing cost etc. [2-6]. Due to the environmental hazard and the toxicity of lead-based perovskite, there is a tremendous effort towards developing Lead-free halide perovskite with improved chemical stability under heat, extended light exposure and humid ambient air. Reference [7] presented a systematic first-principle calculations study of double perovskite,  $\text{A}_2\text{M}^+\text{M}^{3+}\text{X}_6$  with potentially superior photovoltaic performance. Where A is an organic or inorganic component,  $\text{M}^+$  and  $\text{M}^{3+}$  are metal atoms, and X is a halogen atom with band gaps spanning the solar range. They found two In<sup>+</sup>-based compounds,  $\text{Cs}_2\text{InSbCl}_6$  and  $\text{Cs}_2\text{InBiCl}_6$  to have direct optical band gaps of 1.02 eV and 0.91 eV, respectively. And the materials have high theoretical solar cell efficiencies

comparable to that of  $\text{CH}_3\text{NH}_3\text{PbI}_3$  [7]. This report has constituted an important step forward in the design of environmentally friendly perovskite solar cells [8].

Researchers often use the first principle study to model or simulate the electron/hole effective masses, theoretical absorption spectra, carrier mobilities, and energy band gap of materials for technological application [9]. Density functional theory (DFT), a modelling tool has been widely employed for simulating the electronic structures of many-body systems using atomic-scale quantum mechanics [1]. The accuracy of DFT calculations highly depends on the exchange-correlation functionals used. A range of exchange-correlation functionals are available in DFT computations, including Local density approximation (LDA) and generalized gradient approximation (GGA); both have a qualitative impact on the final output. However, this does not rule out the possibility of issues with unexpected cancellations between the exchange-correlation constituents of LDA/PZ and GGA/PBE which may result in unphysical electron self-interactions [10]. This submission

causes both the LDA/PZ and GGA/PBE functionals to significantly underestimate solid band gaps by 30–100% [11]. Despite there being several studies on the properties of lead-free halide perovskite, only very few literatures are available for choosing various DFT exchange-correlation functionals and the different pseudopotential methods for accurate calculations of the structure and properties of lead-free halide perovskites,  $\text{Cs}_2\text{InSbCl}_6$ .

In this work, we investigate and focus mainly on the calculations of crystal structure, lattice parameters, bond length, band structure, density of states (DOS) and partial density of state (PDOS) for  $\text{Cs}_2\text{InSbCl}_6$  using the various DFT functionals and pseudopotential methods. The purpose of this study is to present the DFT calculations and performance of various exchange-correlation functionals in predicting the structural and electronic properties of the lead-free halide perovskite,  $\text{Cs}_2\text{InSbCl}_6$ .

## II. COMPUTATIONAL METHOD

We began with the crystal parameters and atomic positions of Lead-free halide perovskite compound  $\text{Cs}_2\text{InSbCl}_6$  obtained from the Material Projects online database.  $\text{Cs}_2\text{InSbCl}_6$  is a face-centred cubic (FCC) belonging to the space group  $\text{Fm}\bar{3}\text{m}$  [12]. A supercell of 40 atoms was used in the course of this work. A plane-wave (PW) pseudo potential technique as implemented in the Quantum ESPRESSO simulation package within the framework of DFT was used throughout the work. The GGA in the Perdew, Burke, Ernzerhof (PBE) and the LDA in the Perdew Zunger (PZ) [13] was used as the exchange-correlation functionals independently [14]. The Maxfessel-Paxton smearing method was employed for the integrals. The structural parameters (lattice parameters and internal atomic coordinate) were optimized and fully relaxed using Broyden-Fletcher-Goldfarb-Shanno (BFGS) quasi-Newton algorithm. 60 and 240 Ry were set for the convergence test of the kinetic energy cut-off for wave function and charge densities respectively. The Monkhorst-pack-point mesh sampling of Brillouin zone integration was set as  $6 \times 6 \times 6$  and a denser k-point mesh of  $12 \times 12 \times 12$  for density of state (DOS).  $10^{-7}$  was set as the convergence threshold for self-consistent-field (SCF) iteration. The value of pressure,  $P$ , in (1) which was used to calculate the bulk modulus of the material was obtained from the output file of the SCF calculation.

$$\left. \begin{aligned} B_0 &= -V_{av}^{dp} = B_1 + B_2 & (a) \\ B_1 &= -V_1^{(p_1-p_2)} & (b) \\ B_2 &= -V_1^{(p_1-p_3)} & (c) \end{aligned} \right\} (1)$$

## III. RESULT AND DISCUSSION

### A. Structural properties

The crystal lattice parameters ( $\text{\AA}$ ) calculated within LDA/PZ and GGA/PBE functionals compared to available

literature data results for  $\text{Cs}_2\text{InSbCl}_6$  are listed in Table I. The relative deviation between the calculated parameters is also listed to show the performance and diversity in the crystal parameters.

Table I. Crystal lattice parameters (a), relative deviation, average bond length, bulk modulus ( $B_0$ ), calculated by different DFT functionals in this work compared with available literature data results for  $\text{Cs}_2\text{InSbCl}_6$ .

	LDA	GGA	REF
	PZ	PBE	
Lattice parameters (a) $\text{\AA}$	11.28	11.3421	11.32 [15]
Relative deviation (%)	-0.3534	0.195	
Cs-Cl $\text{\AA}$	2.8382	2.9474	
In-Cl $\text{\AA}$	2.5360	2.4655	
Sb-Cl $\text{\AA}$	3.7234	4.1218	
Bulk modulus $B_0$ GPa	27.206	28.45	

The crystal lattice parameters calculated within LDA/PZ and GGA/PBE are  $11.28\text{\AA}$  and  $11.3421\text{\AA}$  respectively. Compared with the available literature value [15], a relative deviation of -0.3534% and 0.195% was noticed for DFT-LDA and DFT-GGA respectively. These deviations may be due to unphysical electron self-interactions [10]. The lattice parameter calculated within GGA/PBE has the least relative deviation compared with the literature data. Fig. 1(a) and (b) show the crystal structure of cubic perovskite within LDA/PZ and GGA/PBE respectively. It shows that the material crystallizes in the cubic  $\text{Fm}\bar{3}\text{m}$  space group. The average bond length for both LDA/PZ and GGA/PBE is listed in Table 1. From Fig. 1,  $\text{Cs}^{1+}$  is bonded to twelve equivalent  $\text{Cl}^{1-}$  atoms. It forms a  $\text{CsCl}_{12}$  cuboctahedron that shares twelve comparable corners of  $\text{CsCl}_{12}$  cuboctahedron, six equivalent faces with  $\text{CsCl}_{12}$  cuboctahedron, six equivalent faces with  $\text{InCl}_6$  octahedral, and six equivalent faces with  $\text{SbCl}_6$  octahedral. The average Cs–Cl bond lengths are  $2.8382\text{\AA}$  in the case of LDA/PZ and  $2.9474\text{\AA}$  for GGA/PBE. Similarly, the  $\text{In}^{1+}$  is bonded to six equivalent  $\text{Cl}^{1-}$  atoms which form  $\text{InCl}_6$  octahedral that share corners with six equivalent  $\text{SbCl}_6$  octahedral and eight equivalent faces with  $\text{CsCl}_{12}$  cuboctahedron. The average In–Cl bond length is  $2.5360\text{\AA}$  in the case of LDA/PZ and  $2.4655\text{\AA}$  for GGA/PBE.  $\text{Sb}^{3+}$  is bonded to six equivalent  $\text{Cl}^{1-}$  atoms to form  $\text{SbCl}_6$  octahedral that share corners with six equivalent  $\text{InCl}_6$  octahedral and eight equivalent faces with  $\text{CsCl}_{12}$  cuboctahedron. The corner-sharing octahedral is not tilted. The average Sb–Cl bond lengths are  $3.7234\text{\AA}$  in the case of LDA/PZ and  $4.1218\text{\AA}$  for GGA/PBE. Finally, the  $\text{Cl}^{1-}$  is found to be bonded in a clear distorted linear geometry to four equivalents  $\text{Cs}^{1+}$ , one  $\text{In}^{1+}$ , and one  $\text{Sb}^{3+}$  atom.

### B. Electronic properties

The results of the band structure calculated by the different DFT functionals and various plane-wave pseudo potential methods for  $\text{Cs}_2\text{InSbCl}_6$  are presented in Table II.

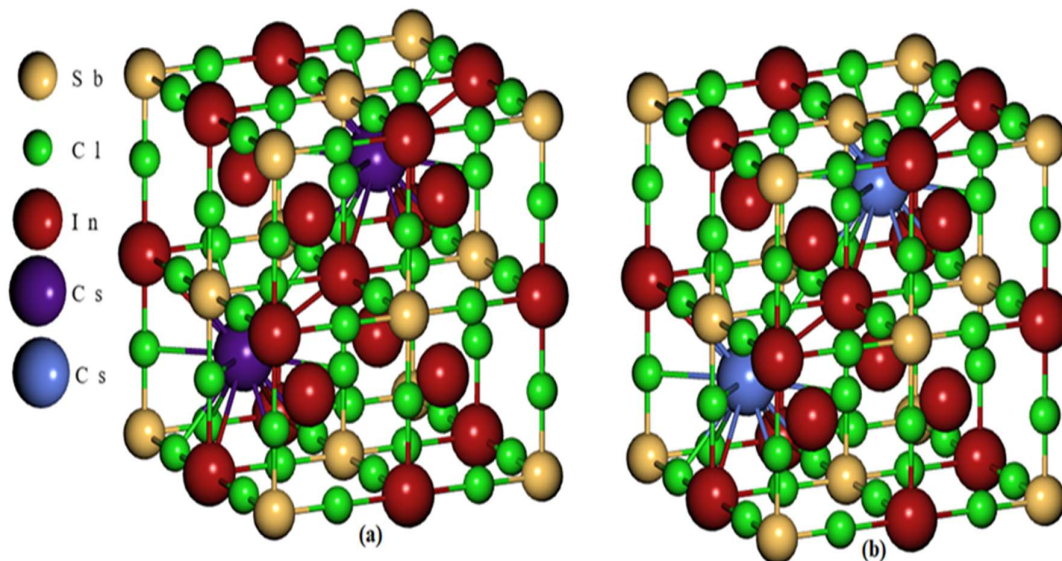


Fig. 1 Optimized Crystal structure (a) With LDA/PZ for  $\text{Cs}_2\text{InSbCl}_6$  (b) With GGA/PBE for  $\text{Cs}_2\text{InSbCl}_6$

The relative deviation between the calculated bands is also listed to show the performance and diversity in the band structure.

Table II. The band gap (in eV) calculated by the different DFT functionals in this work compared with available literature data results for  $\text{Cs}_2\text{InSbCl}_6$ .

	LDA PZ	GGA PBE	REF
Band gap ( $E_g$ ) eV	0.74	0.99	0.98 [16] 1.02 [15]
Relative deviation (%)	-32.43	1.01	

The value of the bandgap is frequently underestimated by LDA/PZ and GGA/PBE [17]. The electronic band gap was calculated employing the two approximations for eventual comparison. The band structure was calculated in the high symmetrical direction of the Brillouin zone (X- $\Gamma$ -W- $\Gamma$ -L) within the LDA/PZ and GGA/PBE. These are presented in Fig. 2(a) and 2(b) for LDA/PZ and GGA/PBE respectively. The zero-energy level was set to coincide with Fermi energy. The band structure of the two approximations reveals that  $\text{Cs}_2\text{InSbCl}_6$  exhibits semiconductor behaviour. Both the LDA/PZ and GGA/PBE have their conduction band minimum and a valence band maximum coinciding at the  $\Gamma$ -point of the Brillouin zone. This indicates that the compound is a direct bandgap material. The plot reveals that the compound has a bandgap of 0.74 eV and 0.99 eV within LDA/PZ and GGA/PBE respectively, the GGA/PBE result is in better agreement with the value of 0.98 eV obtained by [16] and most recently 1.02 eV obtained by [15]. However, they both underestimate the obtained value [17], evidently because of its simplistic form, which isn't flexible enough to regenerate exchange-correlation energy accurately.

The DOS indicates how the material's energy gap behaves. It provides information on the number of possible states in the system, as well as the number of permissible electrons (hole) states per volume at a certain energy level. It's a crucial instrument for evaluating energy distributions and carrier concentrations in semiconductors [18]. Fig. 3(a) and 3(b) show the DOS within DFT-LDA and DFT-GGA respectively. It shows that there is an energy range below and above Fermi's level (0 eV). The higher peaks are located at the valence band, as shown. This suggests that there are a lot of electrons in that energy level. Finally, the DOS supports the material's gap nature, with an energy gap of 0.74 eV for DFT-LDA and 0.99 eV for DFT-GGA with more electrons in the conduction band.

The partial density of state (PDOS) is the relative contribution of a particular atom/orbital to the total DOS. It provides details about the origin of bands both in the valence and conduction bands.

Fig. 4 shows the graph of the PDOS which indicates that the valence band maximum (VBM) is contributed from the Cs-5s orbital. The Cs-5p orbital is associated with the contribution in the conduction band while the Cs-6s have a contribution to both valence and conduction band. The conduction band maximum (CBM) is contributed by the transition In-4d orbital. The In-5s orbital contributed to the conduction band while the In-5p orbital contributed to both the valence and conduction band. The Sb-5s and 5p orbital have most of their contribution to the conduction band. The Cl-5s orbital contributed to both the valence and the conduction band while the Cl-3s had most of its contribution to the conduction band.

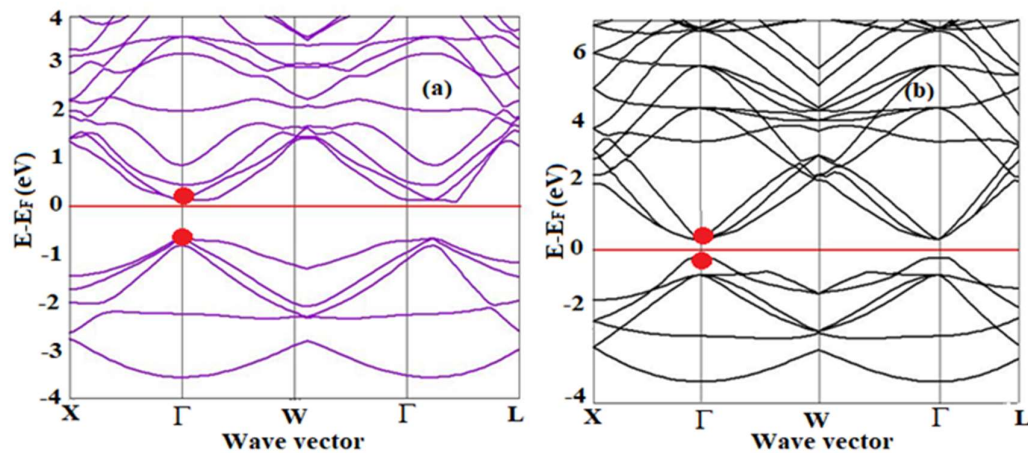


Fig. 2 Calculated Electronic Band structure: (a) with LDA/PZ for  $\text{Cs}_2\text{InSbCl}_6$  and (b) with GGA/PBE for  $\text{Cs}_2\text{InSbCl}_6$

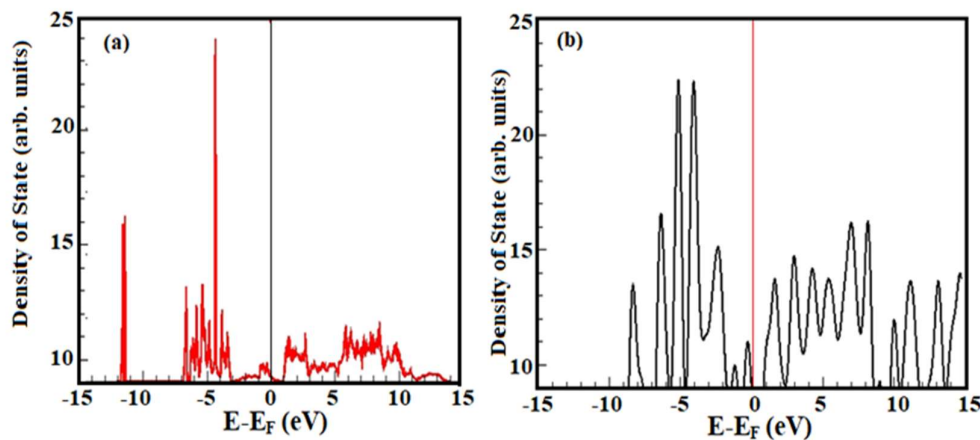


Fig. 3 Calculated Density of state (DOS) (a) with LDA/PZ for  $\text{Cs}_2\text{InSbCl}_6$  and (b) with GGA/PBE for  $\text{Cs}_2\text{InSbCl}_6$

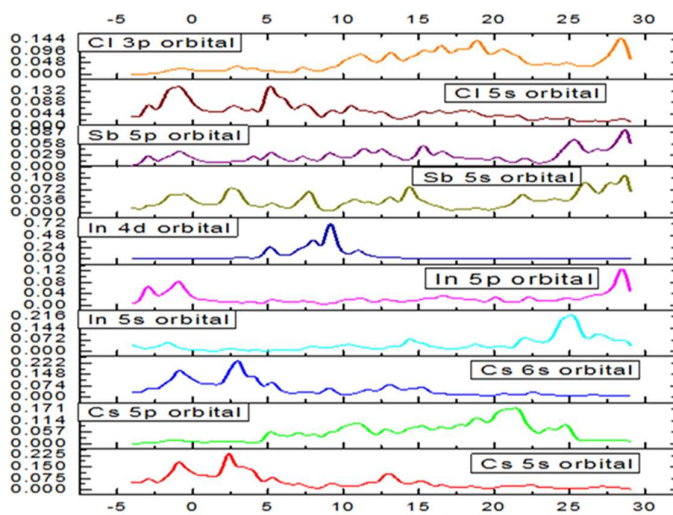


Fig. 4 Partial density of state (PDOS)

## IV. CONCLUSION

Quantum ESPRESSO package runs the different DFT calculation methods on the crystal structure and electronic properties of lead-free double halide perovskite  $\text{Cs}_2\text{InSbCl}_6$  within LDA/PZ and GGA/PBE. The calculated lattice constant, bond length, energy band structure, DOS and PDOS show that GGA/PBE exchange-correlation functional is the best combination of all the density functional methods and pseudo potential in predicting the structural and electronic properties of the lead-free double halide perovskite  $\text{Cs}_2\text{InSbCl}_6$ .

## CONFLICT OF INTEREST

The authors have no known competing financial interests or personal relationships that could have appeared to influence this work.

## Reference

- [1] L. Xiaoming et al., "All inorganic halide perovskites nanosystem: synthesis, structural features, optical properties and optoelectronic applications." *Small*, vol. 13, no. 9, pp. 1603996, 2017.
- [2] G. Giorgi et al., "Small photocarrier effective masses featuring ambipolar transport in methylammonium lead iodide perovskite: a density functional analysis." *The J. of Phy. Chem. Lett.*, vol. 4, no. 24, pp. 4213-4216, 2013.
- [3] Y. Zhao and K. Zhu, "Organic-inorganic hybrid lead halide perovskites for optoelectronic and electronic applications." *Chem. Soc. Rev.*, vol. 45, no.3, pp. 655-689, 2016.
- [4] U. Khan, et al., "Organic-inorganic hybrid perovskites based on methylamine lead halide solar cell. *Sol. Energy*, vol. 189, pp. 421-425, 2019.
- [5] Q. Zhao et al. Stability challenges for perovskite solar cells. *Chem. Nano. Mat.*, vol. 5, no 3, pp. 253-265, 2019.
- [6] R. Wang et al., "A review of perovskites solar cell stability". *Adv. Func. Mat.*, vol. 29, no. 47, pp. 1808843, 2019.
- [7] X. G. et al., "Design of lead-free inorganic halide perovskites for solar cells via cation-transmutation. *J. of the Amer. Chem. Soc.*, vol. 139, no. 7, pp. 2630-2638, 2017.
- [8] S. Alnujaim et al., "Density functional theory screening of some fundamental physical properties of  $\text{Cs}_2\text{InSbCl}_6$  and  $\text{Cs}_2\text{InBiCl}_6$  double perovskites". *The Euro. Phy. J. B*, vol. 95, no. 7, pp.114, 2022.
- [9] P. Umari et al., "Relativistic GW calculations on  $\text{CH}_3\text{NH}_3\text{PbI}_3$  and  $\text{CH}_3\text{NH}_3\text{SnI}_3$  perovskites for solar cell applications". *Sci. Rep.*, vol.4, no. 1, pp. 1-7, 2014.
- [10] S. Somalina, "Electronic properties of GaAs and Hubbard interaction in transition metal oxide." PhD dissertation, Abbrev. Dept., Abbrev. Univ., City of Univ., Abbrev. State, 2012.
- [11] Z. Xiao, Z. Song and Y. Yan, "From lead halide perovskites to lead-free metal halide perovskites and perovskite derivatives". *Adv. Mat.*, vol. 31, no. 47, pp. 1803792, 2019.
- [12] M. R. Filip and F. Giustino, "Computational screening of homovalent lead substitution in organic-inorganic halide perovskites". *The J. of Phy. Chem. C*, vol. 120, no. 1, pp. 166-173, 2016.
- [13] J. P. Perdew, K. Burke and M. Ernzerhof, "Generalized gradient approximation made simple". *Phy. Rev. Lett.* vol. 77, pp. 3865, 1996.
- [14] J. P. Perdew et al., "Atoms, molecules, solids, and surfaces: Applications of the generalized gradient approximation for exchange and correlation". *Phy. Rev. B*, vol. 48, no. 7, pp. 4978, 1993
- [15] Y. Li, "First-Principles Study of Hybrid Halide Perovskites and Beyond for Optoelectronic Applications". PhD dissertation, nano Eng., Univ. Cal., San Diego, 2020.
- [16] Z. Xiao et al., "Intrinsic instability of  $\text{Cs}_2\text{In}(\text{I})\text{M}(\text{III})\text{X}_6$  (M= Bi, Sb; X= halogen) double perovskites: a combined density functional theory and experimental study". *J. of the Amer. Chem. Soc.*, vol. 139, no. 17, pp. 6054-6057, 2017.
- [17] M. Houari et al., "Structural, electronic and optical properties of cubic fluoroelpasolite  $\text{Cs}_2\text{NaYF}_6$  by density functional theory. *Chn. J. of Phy.* vol. 56, no. 4, pp. 1756-1763, 2018.
- [18] N. D. Masters et al., "The impact of subcontinuum gas conduction on topography measurement sensitivity using heated atomic force microscope cantilevers". *Phy. of Fluids*, vol. 17, no. 10, pp. 100615, 2005.